



bone marrow of joints from patients with RA<sup>16</sup>, as well as in inflammatory bone marrow lesions of untreated human tumor necrosis factor (TNF)-transgenic mice with moderate or severe arthritis<sup>17</sup>. These authors' suggestion that synovial inflammatory tissue can break the cortical barrier to reach the adjacent bone marrow is not yet proven. Alternatively, or additionally, as suggested by Bogoch and Moran<sup>18</sup>, proteolytic enzymes may be released into the joint cavity by a trans-osseous process, whereby cytokines and enzymes are released from cells within subarticular bone marrow. The process of juxtaarticular inflammation of marrow spaces and its potential role in articular joint damage has not been fully explored.

Subchondral bone erosions in inflammatory arthritis result from osteoclast activity. Bisphosphonates, which selectively target bone and bind strongly to hydroxyapatite, inhibit osteoclast recruitment and activity<sup>19</sup>. In the rabbit carrageenan-induced arthritis model, administration of the aminobisphosphonates pamidronate or zoledronate inhibits osteoclast activity, increases trabecular bone volume, reduces cortical bone porosity, and increases fracture strength<sup>2,20,21</sup>. Administration of pamidronate prevents thinning and resorption of the subchondral bone plate, which supports the joint surface and separates articular cartilage from underlying marrow, and has a partial protective effect on articular cartilage against destruction by intraarticular inflammatory arthritis<sup>18</sup>.

Histological evaluation of animal models of arthritis and the effects of bisphosphonates has been limited to general measures of inflammation, including: clinical scores for periarticular soft tissue edema<sup>8,11,22-26</sup>; radiographic evaluation of severity of bone and joint destruction<sup>22,24,25</sup>; inflammatory articular changes (i.e., pannus formation and infiltration)<sup>8,11,25</sup>; hematological measures such as erythrocyte sedimentation rates, leukocyte counts in blood smears, or type I collagen crosslinks<sup>8,11,25</sup>; tartrate-resistant acid phosphatase activity-positive cell counts in longitudinal sections<sup>22,25,26</sup>; histological scores for enhanced bone resorption and excessive new bone formation<sup>8,11,25</sup>; general bone erosion scores<sup>23,25,26</sup>; and flow cytometry of bone marrow and peritoneal cells<sup>23</sup>. The histological effects of bisphosphonate treatment on individual cell populations within the bone marrow of animals with arthritis have not been evaluated. The above studies have been limited to the evaluation of clodronate and 3 aminobisphosphonates in collagen-induced and adjuvant arthritis in rats.

In our study, 2 established animal models of inflammatory arthritis, carrageenan-induced arthritis in rats and in rabbits, were evaluated for evidence of intraosseous inflammation. The rat model was studied using flow cytometry to provide confirmation that cell populations indicative of intraosseous inflammation were present in the subchondral bone marrow. The carrageenan arthritis model in the rabbit has been well established and bisphosphonate treatment has

been demonstrated to increase trabecular bone volume and fracture strength<sup>2,21,27</sup>. We used this model to further elucidate histological changes representative of inflammation in the various cell populations of juxtaarticular subchondral bone marrow. This model was used to assess not only the presence and extent of the intraosseous inflammation we hypothesized in arthritis, but also the effect of zoledronate on intraosseous inflammation.

## MATERIALS AND METHODS

**Rats.** Sprague-Dawley rats (125–250 g; Charles River Laboratories, Wilmington, MA, USA) were treated with the sulfated mucopolysaccharide carrageenan (Satiagum B; Sugro, Basel, Switzerland) in sterile solution (1% in normal saline) via intraarticular injection (8  $\mu$ l/100 g rat weight) of the right tibiofemoral joint to induce arthritis. Seven injections were administered to each animal over 24 days as described<sup>28</sup>. Animals were divided into 2 groups (n = 9 each group): normal saline only controls (N) and arthritis (A).

On Day 24, 2.5 ml peripheral blood samples were collected and the animals were euthanized. The femur was surgically removed, and the femoral head and distal femoral condyles were removed. The femur was flushed out with 0.1 M phosphate buffered saline with 0.5% fetal calf serum (PBS 0.5% FCS), and the extruded cellular material was collected and kept on ice. The spleen was removed and its cellular contents were collected by teasing the spleen on a filter and then kept on ice.

Harvested marrow and spleen cells were washed by topping the collected volume up to 15 ml using PBS 0.5% FCS, followed by centrifugation (10 min, 1250 rpm). The resultant pellets were resuspended in 2 ml (marrow) or 3 ml (spleen) of ACK (0.155 M ammonium chloride, 0.1 mM disodium EDTA, 0.01 M potassium bicarbonate). Peripheral blood was treated with 2 ml of ACK. After 3 min incubation on ice, each sample was topped up to 15 ml with PBS 0.5% FCS and centrifuged (10 min, 1250 rpm). The cells were resuspended, incubated, and washed another 3 times prior to resuspension in a small volume of PBS 0.5% FCS.

Staining solutions were prepared by diluting twice the required final concentration of the antibody (Table 1) into the staining buffer (PBS 0.5% FCS, 0.1% NaN<sub>3</sub>), for single and dual color staining and appropriately paired isotype controls. Samples were resuspended to a concentration of 2  $\times$  10<sup>7</sup> cells/ml in PBS 0.5% FCS and stained for each antibody combination and the appropriate controls. Each sample was treated with 5  $\mu$ l normal

Table 1. Antibodies used (source: PharMingen).

Name and Specificity	Catalog No.	Isotype	Other Details
Biotin anti-rat CD3	22012D	IgG3	
Biotin anti-rat mononuclear phagocyte	22452D	IgG1	
Biotin mouse IgG3 anti-fructosan	03062C	IgG3	Isotype control for 22012D
Biotin mouse IgG1 anti-TNP	03002C	IgG1	Isotype control for 22452D
Streptavidin Cy-Chrome	13038A		
R-PE anti-rat CD4	22025B	IgG2a	
R-PE mouse anti-TNP	03025A	IgG2a	Isotype control for 22025B
R-PE anti-rat CD8a	22075B	IgG1	
R-PE mouse anti-TNP	03005A	IgG1	Isotype control for 22075B
FITC anti-rat CD11b/c	22084D	IgG2a	
FITC mouse anti-TNP	03024C	IgG2a	Isotype control for 22084D

human serum to block the Fc receptor and incubated at 37°C for 15 min. Staining solutions (50 µl) were then added to the samples, which were incubated 30 min at 4°C in the dark. Samples were then centrifuged and washed twice in 150 µl staining buffer. Cells were resuspended in 100 µl staining buffer containing streptavidin cytochrome or staining buffer alone. Samples were then incubated (30 min, 4°C, in the dark), washed another 3 times, and resuspended in 500 µl PBS for data acquisition.

Counting was performed on a FACStar Plus flow cytometer (Becton Dickinson, Mississauga, ON, Canada) with the manufacturer's recommended settings using Trypan blue exclusion. Flow cytometry data were collected for each sample until either 20,000 events or exhaustion of the sample tube. Data files were collected and analyzed using the FlowJo software package (Tree Star Inc., San Carlos, CA, USA), gating first for scatter properties most consistent with either lymphocytes or macrophages and then by gating for fluorescence intensity, depending on the fluorochrome of interest. Double-stained populations were compared against each other using a 2-tailed T-test.

**Rabbits.** Experimental inflammatory arthritis was induced in the right tibiofemoral joint of female NZW rabbits weighing 3.6 to 4.5 kg, via intraarticular injection of 0.3 µl of the sulfated mucopolysaccharide carrageenan (Satiagum B; Sugro) in sterile solution (1% in normal saline). A total of 10 injections were administered to each animal over a 7 week period. Sixty animals were divided into 5 groups (n = 12 each group): normal untreated controls that received intraarticular injections of saline (N), arthritis (A), and bisphosphonate-treated from initiation (A+BP0), 2 weeks after initiation (A+BP2), and 4 weeks after initiation (A+BP4) of arthritis induction. Bisphosphonate treatment consisted of daily subcutaneous injection of zoledronate (CGP 42'446; Novartis Pharmaceuticals, Dorval, QC, Canada) at a dose of 3 µg/ml/kg. The protocol was approved by The Wellesley Central Hospital Animal Care Committee.

After 7 weeks, all animals were euthanized, the femora excised, and the distal femoral condyles decalcified, processed and sectioned. Posteromedial femoral condyles were cut longitudinally in the sagittal plane and oriented through the center of the articulating surface into sections 4–5 µm thick, which were subsequently stained with Safranin O Fast Green.

One section from each femur, for a total of 60 sections, was examined by one author (VLF), a bone and joint pathologist, using a Leitz DMRB light microscope at 100× and 500× magnification. The pathologist was blinded to the identity of the specimens, which were evaluated in random order.

An eyepiece graticule bearing a 10×10 matrix was overlaid on each section and aligned parallel to the tidewater mark, resulting in an analysis area of 3 mm × 3 mm that included the posterior (adjacent to pannus), middle (non-weight-bearing), and anterior (functional weight-bearing) zones. The analysis area on each section ranged from 56 to 157 squares, with means of 130.5 (N), 77.0 (A), 94.5 (A+BP0), 82.5 (A+BP2), and 106.0 (A+BP4) squares (n = 12 each condition).

Each square in a section was analyzed for several cell types and histological features relevant to inflammation, which were evaluated and assigned a categorical grade ranging from 0 to 3, a grade of 0 indicating normal, healthy tissue morphology, and a grade of 3 indicating "abnormal" morphology as typically seen in extensive inflammation (Table 2). The cell types and histological features relevant to inflammation that were graded categorically included: vascularity, fibrosis, fibrocytes, lipocytes, hematopoietic activity, lymphocytes, plasma cells, polymorphonuclear (PMN) cells, histiocytes, mononuclear cells, giant cells, and foamy cells. The "tidemark" (interface of calcified/uncalcified cartilage) was evaluated on a continuous scale, expressed as the number of grid squares where tidemark was intact.

The categorical grades assigned to each cell type and histological feature examined were recorded for each square in all sections within the 5 groups (N, A, A+BP0, A+BP2, A+BP4). For each cell type and histological feature, the total number of squares for each grade (0, 1, 2, 3) was then calculated and expressed as a percentage of the total number of squares within the treatment group. The data were considered for the 5 treatment

groups, and also by pooling the data for the 3 zoledronate-treated groups (BP, n = 36).

The categorical data were evaluated by nonparametric analysis, using the Kruskal-Wallis test, followed by Mann-Whitney U tests for pairwise comparisons of interest: N versus A, A versus A+BP0, A versus A+BP2, A versus A+BP4, and A versus BP.

For the continuous data (tidemark), means and standard deviations were calculated for each of the 5 treatment groups. To test intraobserver agreement, 10 slides were evaluated in one session, and then reevaluated by the same observer in a different session at a later date, after having examined other slides in the interim. Eleven histological indicators of inflammation were evaluated: vascularity, fibrosis, fibrocytes, lipocytes, hematopoietic activity, lymphocytes, plasma cells, PMN cells, histiocytes, mononuclear cells, and tidemark. The kappa statistic was calculated to determine the level of agreement for each of these indicators, according to the scale originally proposed by Landis and Koch<sup>29</sup>, who interpreted values of 0 to 0.2 as slight agreement, 0.2 to 0.4 as fair, 0.4 to 0.6 as moderate, 0.6 to 0.8 as substantial, and > 0.8 as almost perfect agreement.

## RESULTS

**Rats: flow cytometry.** Physical signs of arthritis were observed in the carrageenan-induced arthritis rats, including visible swelling of the hind limbs and reduced ambulatory function, whereas untreated rats showed no signs. Flow cytometry was utilized in this model to provide an indication of inflammation.

The relative numbers of CD3+CD4+ lymphocytes, CD3+CD8+ lymphocytes, and CD11b/c+MNP+ monocytes in bone marrow, blood samples, and spleen extracts of carrageenan-induced arthritis rats and control rats, as assessed by flow cytometry, are shown in Table 3. The percentages of CD3+CD4+ lymphocytes (Figure 1) and CD11b/c+MNP+ monocytes (Figure 2) were significantly elevated in the bone marrow of arthritic rats compared to normal rats (p = 0.04, p = 0.0002, respectively; Table 3), consistent with intraosseous inflammation. The increase in CD4+ T cells (Figure 1) and CD11b/c+MNP+ monocytes (Figure 2) was specific to bone marrow; no corresponding increase was observed in peripheral blood or spleen. There were no significant changes in CD8+ T cells in any samples.

**Rabbits: histology.** To further elucidate the presence of intraosseous inflammation in arthritis and the effect of bisphosphonates on this process, we induced inflammatory arthritis in rabbits by intraarticular carrageenan injection. This model is useful for histological analysis, as the effects of bisphosphonates on osteoclast activity and cortical bone density in carrageenan-induced arthritis in rabbits are well established<sup>2,20,21</sup>.

In inflammatory arthritis, there was marked thinning of the tidemark and perforation by marrow cells, with exposure of articular cartilage (Figure 3). Histologic evidence of inflammation in the arthritic specimens included groups of lymphocytes, fibrocytes, and mononuclear cells and patchy to extensive fibrosis (Figure 4). The bone marrow appeared normal in bisphosphonate-treated samples in comparison to the untreated arthritis samples (Figure 3), with only individual lymphocytes evident (Figure 4).

Table 2. Histological grading system for categorical variables.

Cell or Tissue Type	“Normal” (no inflammation) 0	Interpretation of Grade →		“Abnormal” (extensive inflammation) 3
		1	2	
Vascularity	None	Distention	Increased number of vessels	Proliferation of endothelial cells
Fibrosis	None	Occasional	Patchy	Extensive
Fibrocytes	None	Medium; individual cells	Moderate; groups of cells	Marked; masses of cells
Lipocytes	Intact	Lipocytes predominate with islands of fibrosis/inflammation	Lipocytes separated by fibrosis/inflammation	Absent, replaced by fibrosis/inflammation
Hematopoietic cells	Individual cells occupy ≤ 50% of area	Decreased	Substantially decreased, with fibrosis/inflammation	Absent, replaced by fibrosis/inflammation
Lymphocytes	None	Medium; individual cells	Moderate; groups of cells	Marked; masses of cells
Plasma cells	None	Medium; individual cells	Moderate; groups of cells	Marked; masses of cells
Polymorphs	None	Medium; individual cells	Moderate; groups of cells	Marked; masses of cells
Histiocytes	None	Medium; individual cells	Moderate; groups of cells	Marked; masses of cells
Mononuclear	None	Medium; individual cells	Moderate; groups of cells	Marked; masses of cells
Giant	None	Medium; individual cells	Moderate; groups of cells	Marked; masses of cells
Foamy	None	Medium; individual cells	Moderate; groups of cells	Marked; masses of cells

Table 3. Flow cytometry analysis. The Arthritis and Normal columns show the percentage of double-stained cells. P (T ≤ t) is the probability that the differences between arthritic and normal are due to chance, calculated using a 2-tailed T test.

	CD3/CD4 Lymphocytes		CD3/CD8 Lymphocytes		CD11/MNP Monocytes	
	Arthritis	Normal	Arthritis	Normal	Arthritis	Normal
Marrow	0.46* SD 0.25 (n = 9)	0.21, SD 0.21 (n = 9)	0.68, SD 0.36 (n = 7)	0.55, SD 0.20 (n = 8)	14.73* SD 4.80 (n = 7)	3.92, SD 2.64 (n = 7)
p (T ≤ t)	0.04		0.40		0.0002	
Blood	42.33, SD 13.92 (n = 9)	44.64, SD 10.41 (n = 8)	16.71, SD 8.07 (n = 8)	16.16, SD 6.64 (n = 8)	47.77, SD 21.25 (n = 7)	31.20, SD 17.63 (n = 7)
p (T ≤ t)	0.71		0.88		0.14	
Spleen	30.18, SD 8.98 (n = 8)	27.32, SD 9.84 (n = 9)	12.58, SD 5.92 (n = 8)	14.79, SD 4.82 (n = 8)	2.55, SD 1.66 (n = 7)	1.11, SD 1.48 (n = 7)
p (T ≤ t)	0.54		0.43		0.11	

\* Significantly different from normal.

Tests for intraobserver reliability indicated almost perfect agreement for fibrosis ( $\kappa = 0.85$ ) and moderate agreement for plasma cells ( $\kappa = 0.58$ ), mononuclear cells ( $\kappa = 0.58$ ), lipocytes ( $\kappa = 0.48$ ), tidemark ( $\kappa = 0.48$ ), lymphocytes ( $\kappa = 0.41$ ), and PMN cells ( $\kappa = 0.43$ ). Fibrocytes showed fair intraobserver agreement ( $\kappa = 0.36$ ). Histiocytes, vascularity, and hematopoietic activity showed minimal intraobserver agreement ( $\kappa = 0.10$ ,  $\kappa = 0$ ,  $\kappa = 0$ , respectively) and were excluded from further analysis.

Six histological categories with sufficient intraobserver reliability (fibrosis, lipocytes, lymphocytes, plasma cells, PMN cells, mononuclear cells) were graded from 0 (normal) to 3 (abnormal; extensive inflammation; Table 2) in each specimen. The percentage of grade 0, 1, 2, and 3 of each histological category was calculated for the normal, arthritis,

and 3 BP treatment groups (Figure 5). For example, in normal bone marrow, 95% of fibrocytes were identified as grade 0 and the remainder were categorized as grade 1. However, while only 15% of the bone marrow in arthritis had grade 0 fibrocytes, 46% had grade 1, 34% had grade 2, and 5% had grade 3 fibrocytes, indicative of inflammation. The histology of the normal, arthritis, and 3 BP treatment groups varied significantly, as determined by Kruskal-Wallis test, for lymphocytes ( $p = 0.0003$ ), mononuclear cells ( $p < 0.0001$ ), fibrocytes ( $p < 0.0001$ ), fibrosis ( $p < 0.0001$ ), lipocytes ( $p = 0.0006$ ), and plasma cells ( $p = 0.0330$ ). The results were similar when the 5 treatment groups (N, A, A+BP0, A+BP2, A+BP4) were analyzed individually, and when the data for the 3 bisphosphonate-treated groups (A+BP0, A+BP2, A+BP4) were pooled (BP).

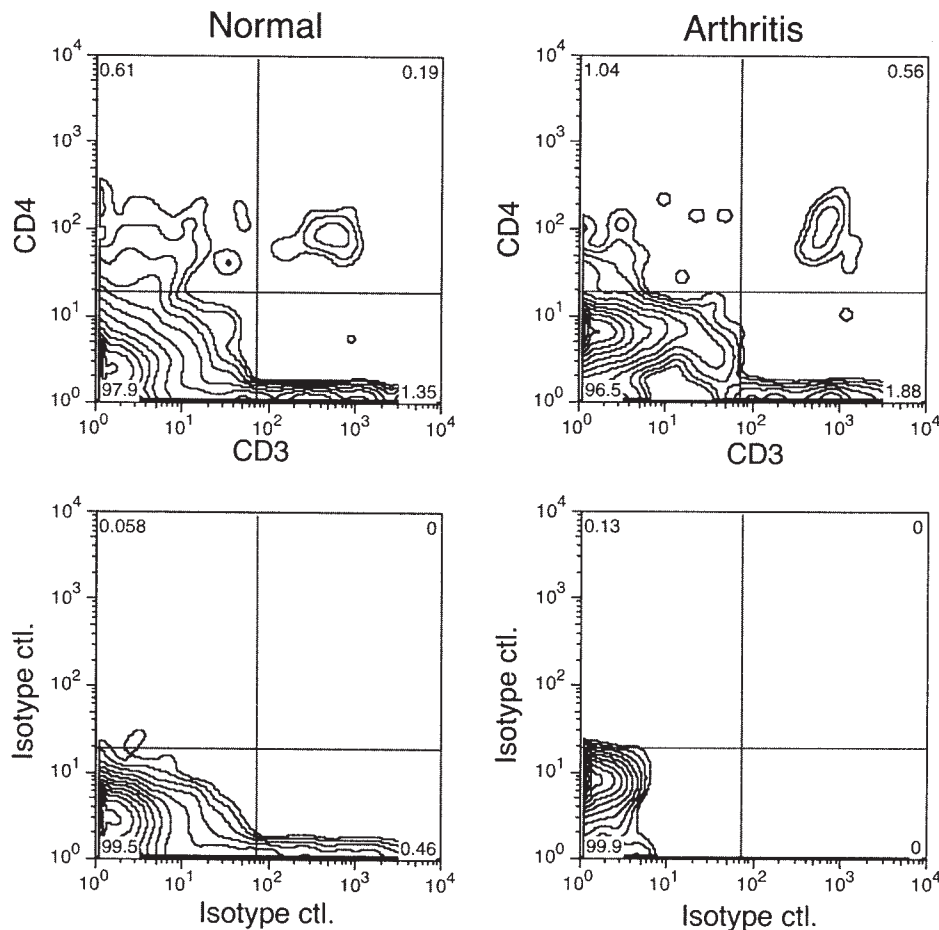


Figure 1. Topographic representation of CD3+CD4+ lymphocytes costained for bone marrow from normal (top left panel) and arthritic (top right) rats, and appropriately matched isotype matched controls (bottom row; see Table 1). In bone marrow, CD3+CD4+ lymphocytes were significantly elevated in arthritis (top right) compared to normal (top left; see Table 3).

Comparison of the untreated arthritis and normal groups, by Mann-Whitney U tests, indicated a significant difference in percentages of categorical grades for lymphocytes ( $p = 0.0002$ ), mononuclear cells ( $p < 0.0001$ ), fibrocytes and fibrosis ( $p = 0.0004$ ), lipocytes ( $p = 0.0006$ ), and plasma cells ( $p < 0.005$ ) in the bone marrow. The untreated arthritis samples consistently displayed a shift of 1 to 2 grades higher toward “abnormal” histology, or inflammation, i.e., a significantly greater percentage of these cell types and histological features in sections of the arthritis specimens exhibited a histology typical of inflammation. When the bisphosphonate-treated arthritis group was compared to the untreated arthritis group (Mann-Whitney U test), the mononuclear cell, fibrocyte, fibrosis, and lipocyte categories were significantly altered toward normal ( $p < 0.005$ ,  $p < 0.005$ ,  $p < 0.05$ , and  $p < 0.05$ , respectively, vs arthritis). A greater percentage of these cell types and histological features in the sections of the bisphosphonate-treated specimens displayed a histology consistent with normal bone marrow when compared to sections of the arthritis specimens.

The mean values for intact tidemark for normal, untreated arthritis, and 3 BP-treated arthritis groups are shown in Figure 6. Intact tidemark was reduced in arthritis samples, but showed a significant shift toward normal with each of the 3 durations of bisphosphonate treatment. The results were similar when the data for the 3 bisphosphonate-treated arthritis groups were pooled.

## DISCUSSION

Flow cytometry results showing elevated levels of CD4+ T cells and CD11b/c+MNP+ monocytes confirmed the presence of inflammation within the bone marrow of carrageenan-induced arthritic rat femora. The number of CD4+ lymphocytes was approximately double that found in normal controls, consistent with a previous report of elevated levels of CD4+ T cells in knee synovial membranes from rats with adjuvant arthritis<sup>30</sup>.

Subsequent histological evaluation of individual cell populations in the marrow spaces of subchondral bone of rabbits with carrageenan-induced arthritis revealed signifi-

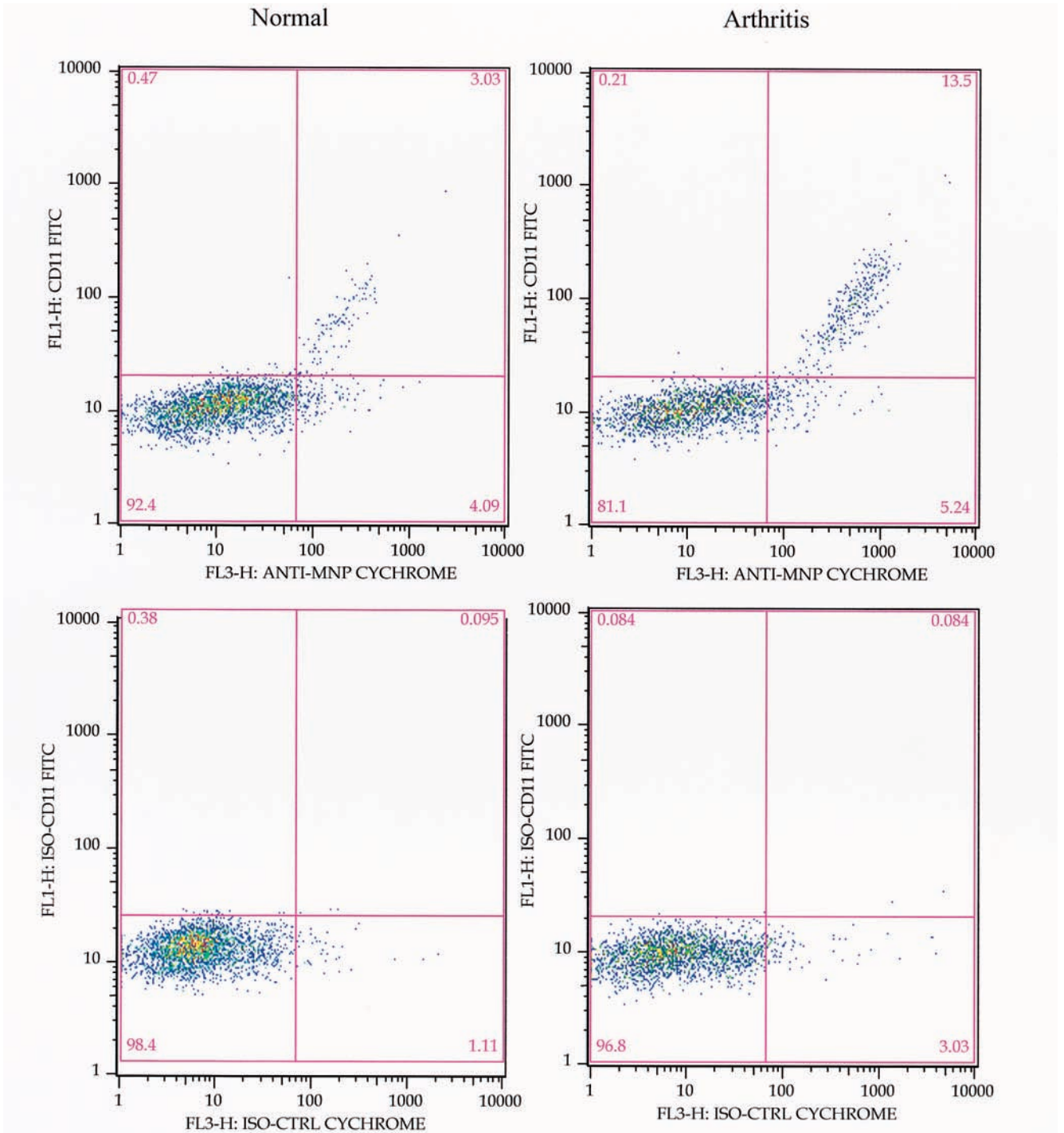
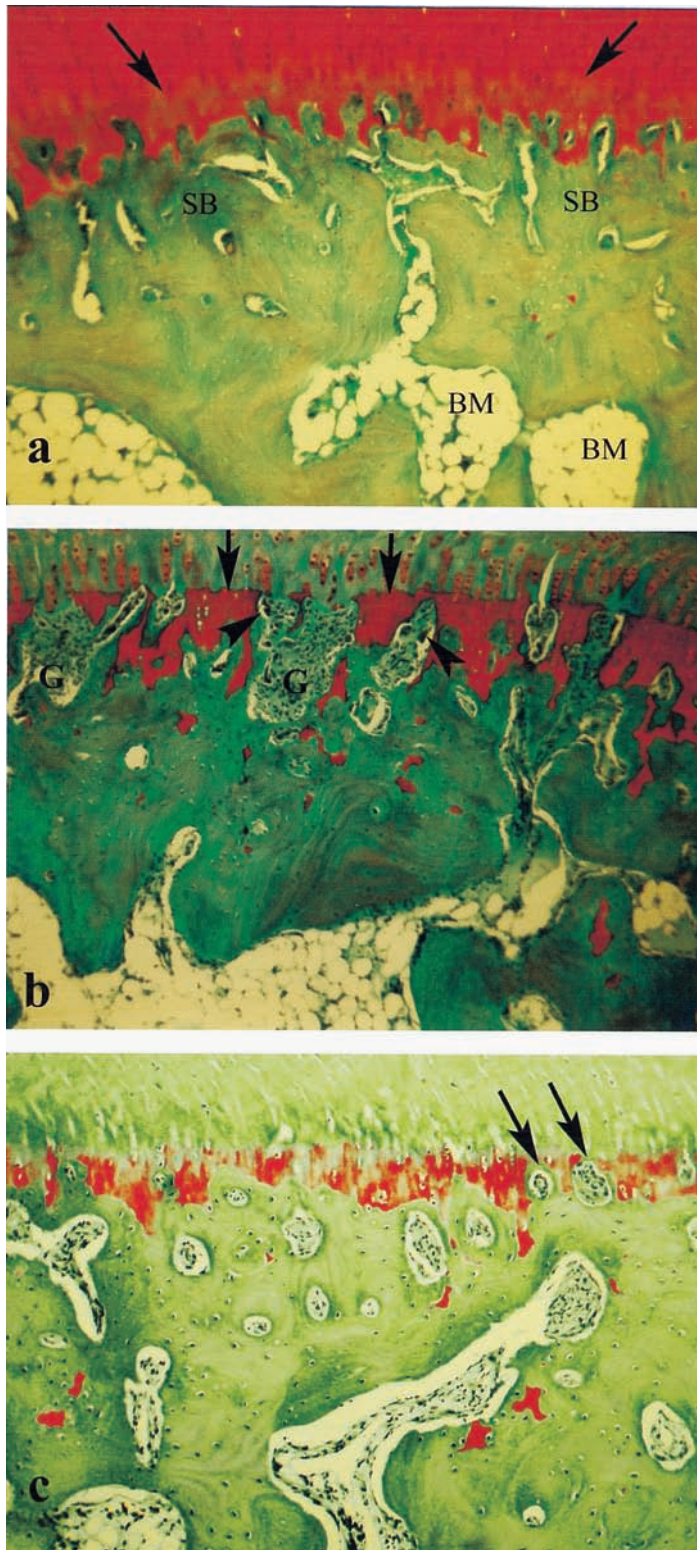


Figure 2. CD11b/c+ anti-MNP+ monocytes in bone marrow: normal sample (left panels), arthritic sample (right panels). The top panels show staining with CD11b/c and anti-MNP (biotin anti-rat mononuclear phagocyte) antibodies; lower panels show staining with appropriate isotype controls (see Table 1). In bone marrow, CD11b/c+ anti-MNP+ monocytes were significantly elevated in arthritis (top right) compared to normal (top left; see Table 3).

cantly elevated levels of lymphocytes, mononuclear cells, plasma cells, fibrocytes, and fibrosis compared to normal samples, and reduced levels of lipocytes, indicating the presence of intraosseous inflammation.

Previous studies of carrageenan-induced arthritis in rabbits have demonstrated a 4-fold increase in osteogenesis<sup>3</sup>

and a 5- to 6-fold increase in bone resorption<sup>4</sup>, resulting in increased bone turnover, osteoporosis, and porosity of cortical bone<sup>4</sup>. There was a significant loss of cancellous bone, a significant decrease in bone volume and trabecular thickness, and an increase in osteoid indicators in the metaphysis. In contrast, in the diaphysis, a significant decrease in corti-



*Figure 3.* Sagittal sections of rabbit distal femoral condyle, decalcified, stained with Safranin O Fast Green. The articular surface lies just outside this view, at the top of the section. Original magnifications 100 $\times$ . Panel (a): Normal. Cascades of healthy chondrocytes are seen in the cartilage (red). Note the subchondral bone (SB) and bone marrow (BM). The SB plate separates cartilage from BM. Calcified cartilage appears as a slightly darker band of cartilage just above the SB plate. The barely visible tidemark (arrows) denotes the junction between calcified and noncalcified cartilage. (b) Arthritis (49 days). The staining characteristics of the uncalcified (articulating) cartilage matrix have changed from red to green, indicating loss of mucopolysaccharide content. Cartilage is more cellular and less organized. Vascular granulation tissue (G) composed of blood vessels and inflammatory cells breaches the bone plate extending from the bone marrow to cartilage, penetrating through the tidemark (arrows). The mineralized cartilage remains stained red below the residual tidemark. The endosteal surfaces are scalloped, indicative of active resorption, and osteoclasts can be identified (arrowheads). (c) Bisphosphonate-treated sample, commenced with initiation of arthritis. The uncalcified cartilage has lost its mucopolysaccharide and is stained green, whereas the calcified cartilage retained its mucopolysaccharide and is stained red. The loss of Safranin O staining and chondrocyte morphological changes indicate cartilage damage. In bone vascular spaces in the bone plate, there is less inflammation than in active disease; small interruptions of the interface between the bone and mineralized cartilage remain (arrows). Cellular perforation of the tidemark (arrows) is reduced in comparison to the arthritis sample. The bone marrow is cellular, but the endosteal surfaces are smoother, with less evidence of active resorption.

cal bone thickness and cancellous bone volume and diameter and a marginal increase in porosity were observed<sup>4,31</sup>. Experimentally induced arthritis also increased osteoclastic and osteoblastic activity in juxtaarticular bone<sup>4</sup>.

Monocytes are precursors of osteoclasts<sup>12,32</sup>, and in our study an increased number of monocytes was observed in the sections of untreated arthritis rabbit femora, and also in the bone marrow of carrageenan-induced arthritic rat femora.

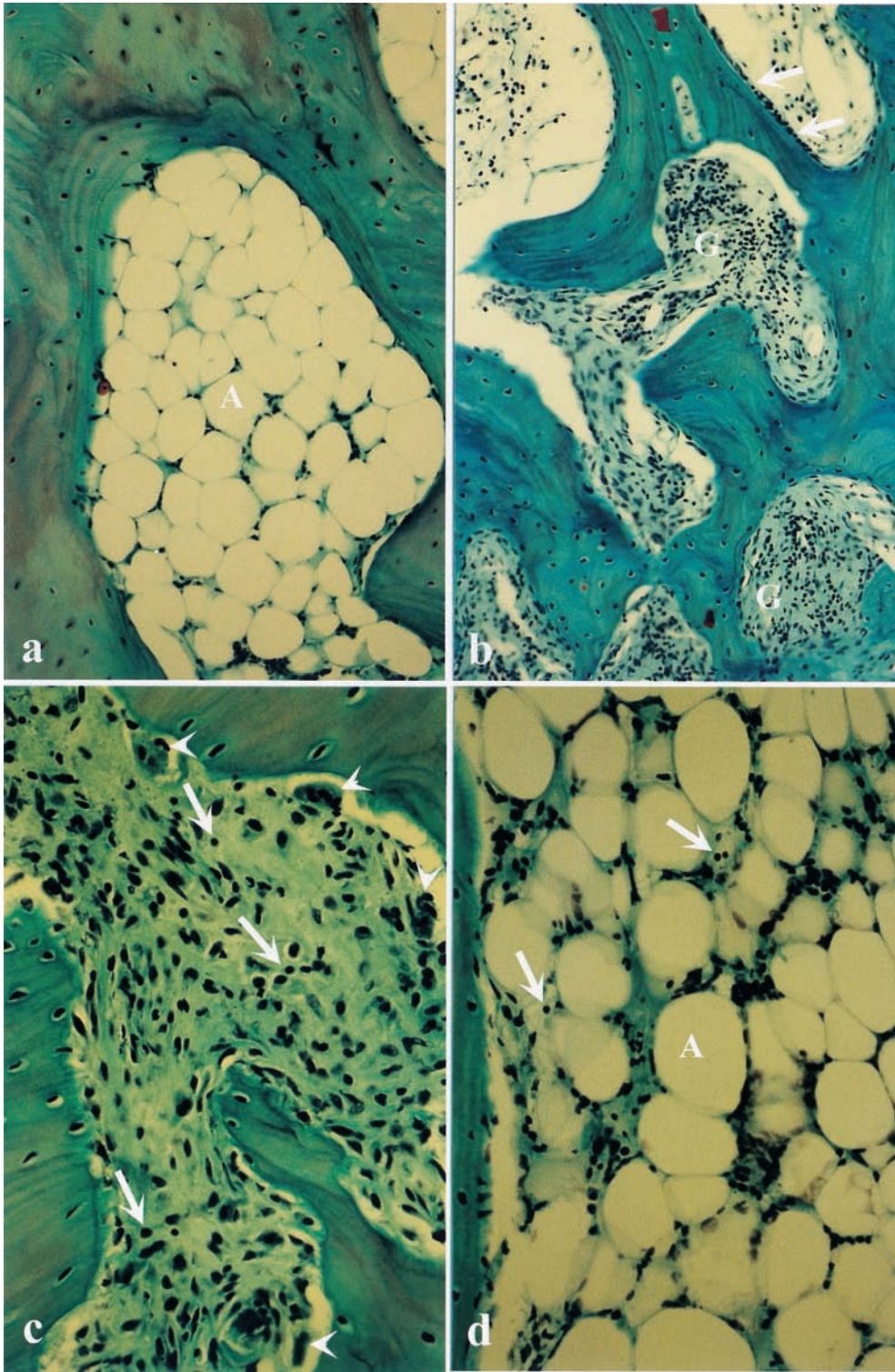


**Figure 4.** Sagittal sections of bone marrow of trabecular bone, immediately subchondral to the cartilage, of rabbit distal femoral condyle, decalcified, stained with Safranin O Fast Green. Original magnifications: (a) 150 $\times$ , (b) 100 $\times$ , (c) 250 $\times$ , (d) 200 $\times$ . (a) Normal. Lipocytes (A) occupy most of the marrow cavity, limited hematopoietic activity. Osteocytes are widely distributed in the bone trabeculae. The endosteal surface is smooth with minimal evidence of osteoblastic or osteoclastic activity. (b) Arthritis (49 days). The bone marrow is occupied by vascular granulation tissue (G), which replaces the lipocytes, and is sprinkled with lymphocytes. The endosteal surface shows active cuboidal osteoblasts with rounded nuclei (arrows). (c) Arthritis (49 days). Higher magnification of bone and bone marrow; bone trabeculae are undergoing a destructive, erosive process. Marrow is occupied by inflammatory cells such as lymphocytes (arrows). Note the osteoclasts and bone resorption at endosteal trabecular margins (arrowheads). (d) Bisphosphonate-treated sample, commenced 2 weeks after initiation of arthritis. Bone marrow appears partially restored to normal in comparison to the changes due to arthritis seen in panel c. Intact lipocytes (A) are evident. Minimal residual vascular granulation tissue and only occasional lymphocytes (arrows) are evident. Note the inactive endosteal surface along the left margin of the photograph.

This may explain the elevated osteoclast populations observed in arthritis. Systemic activation of T cells has been shown to lead to *in vivo* osteoclastogenesis and bone loss mediated by osteoprotegerin ligand (OPGL) in adjuvant arthritis<sup>33</sup>, resulting in further elevation of osteoclast activity.

Treatment with zoledronate has been shown to reduce the percentage of total bone area with defects from that seen in experimental inflammatory arthritis in rabbits to a level similar to that seen in normal specimens<sup>21</sup>. Zoledronate and another bisphosphonate, pamidronate, have also been shown

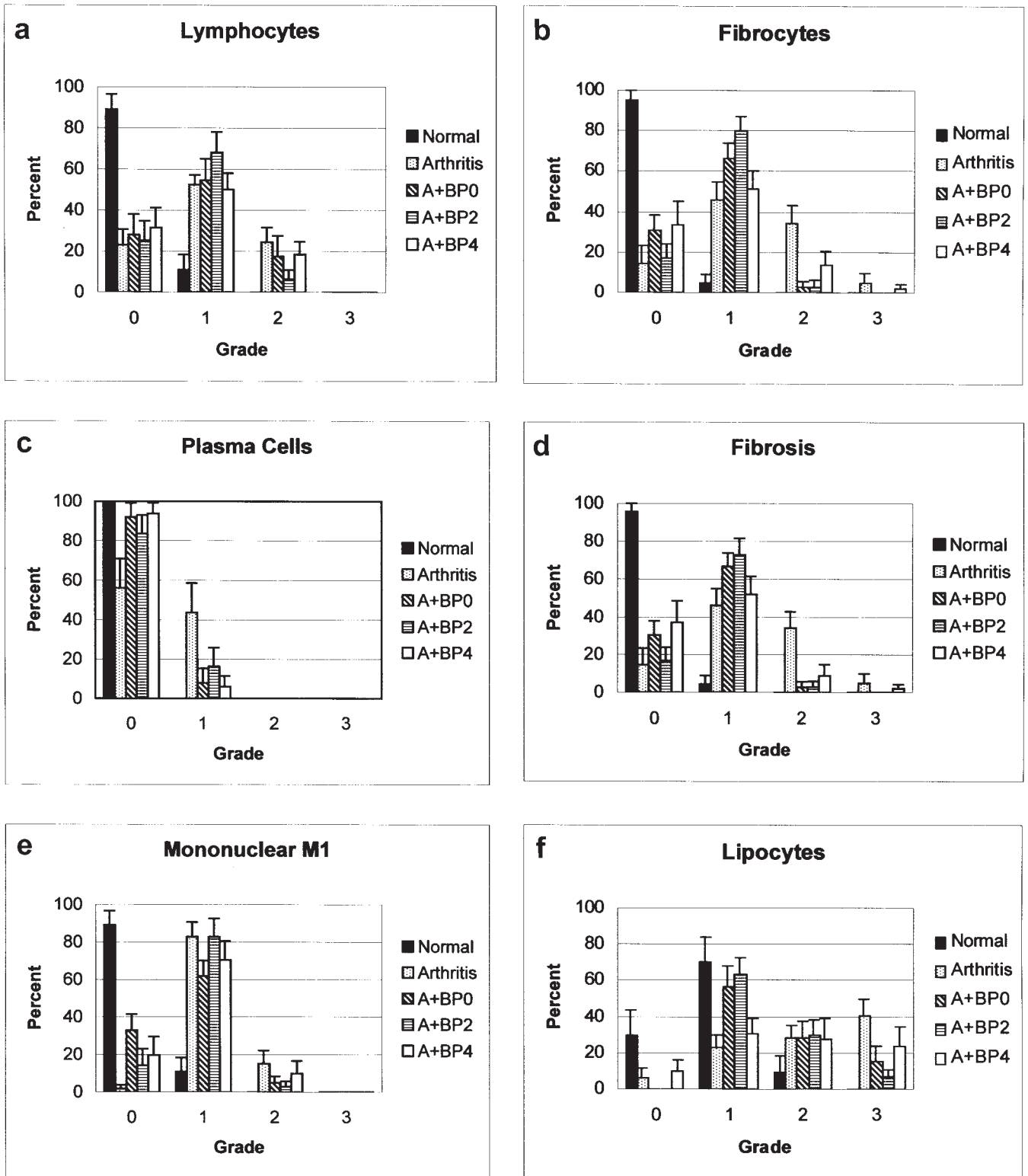


Figure 5. Percentage of cell type or histological feature relevant to inflammation with histological grading of 0 (normal; healthy) to 3 (abnormal; extensive inflammation) in the sections of normal, arthritis, and 3 bisphosphonate treatment groups for (a) lymphocytes; (b) fibrocytes; (c) plasma cells; (d) fibrosis; (e) mononuclear cells; and (f) lipocytes.

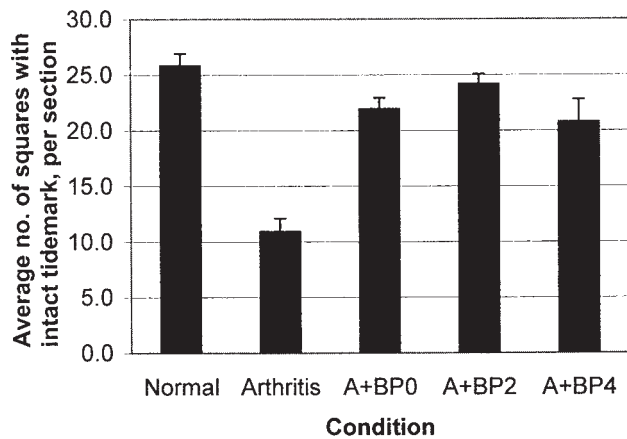


Figure 6. Histological analysis of intact tidemark for normal, arthritis, and 3 bisphosphonate treatment groups.

to increase cancellous bone accumulation in rats<sup>34</sup> and in human TNF-transgenic mice<sup>26</sup>. The effects of pamidronate on cancellous bone in the carrageenan arthritis rabbit model were evaluated by examination of bone volume, new bone volume, trabecular width, and cellular measures such as osteoid perimeter, resting perimeter and percentage of eroded perimeter<sup>27</sup>. Total bone volume was reduced in arthritis compared to normal and was altered toward normal by treatment with pamidronate. This change was attributed to a decrease in osteoclastic resorptive activity, but not to any measurable change in rates of formation or recruitment, since osteoclast number was increased in arthritis, as well as in a dose-dependent manner with pamidronate treatment. In contrast, osteoblast activity was significantly suppressed by pamidronate treatment.

In our study, bisphosphonate treatment of arthritic rabbits significantly altered the histology of mononuclear cells, fibrocytes, fibrosis, and lipocytes in arthritic bone marrow toward normal, suggesting a reduction in the level of chronic bone marrow inflammation. This effect of bisphosphonate treatment in reducing inflammation in bone marrow in arthritis was consistent, whether bisphosphonate treatment was initiated at induction of arthritis (A+BP0) or 2 weeks (A+BP2) or 4 weeks (A+BP4) after induction. Within the limitations of this experimental model, there was no significant difference in the reduction of inflammation between what could be considered to be bisphosphonate “prophylaxis” (A+BP0) versus “treatment” (A+BP2, A+BP4).

The issue of antiinflammatory versus proinflammatory properties of bisphosphonates is complex and is reported to depend upon the presence in the molecules of a nitrogen atom in a specific configuration and distance from the phosphonate group. Several *in vitro* studies and a few acute *in vivo* studies indicate that non-aminobisphosphonates (e.g., clodronate, etidronate) have antiinflammatory effects, suppressing production of proinflammatory cytokines including interleukin 1 (IL-1), IL-6, and TNF- $\alpha$ , and reducing nuclear

factor- $\kappa$ B binding activity<sup>35-42</sup>. Evidence suggesting that aminobisphosphonates (pamidronate, alendronate, risedronate, zoledronate) are proinflammatory and enhance cytokine secretion is reviewed by Maksymowych<sup>39</sup>; and yet pamidronate suppressed IL-1 production in peripheral blood monocytes of RA patients *in vitro*<sup>43</sup>, and RA patients treated with alendronate had significantly lower serum concentrations of IL-1, IL-6, and TNF<sup>44</sup>. The paradoxical effect of bisphosphonates on inflammation is reviewed by Goldring and Gravalles<sup>45</sup>.

A few human studies have focused on various laboratory markers of inflammation, including erythrocyte sedimentation rate and C-reactive protein, in contrast to solely clinical indices of disease severity. Some of these studies have documented an antiinflammatory effect of aminobisphosphonates<sup>43,44,46</sup>, whereas others have indicated an acute proinflammatory effect<sup>47</sup>.

Whereas aminobisphosphonates have been observed to be principally proinflammatory, and non-aminobisphosphonates antiinflammatory, our observations in bone marrow demonstrate antiinflammatory effects of zoledronate, a potent aminobisphosphonate. Previous studies of inflammatory effects of aminobisphosphonates were performed in synovium<sup>9,10,20,25,26</sup>, circulating blood cells<sup>10,39</sup>, and various cell cultures including T cells and PBMN cells<sup>39</sup>, but to our knowledge this is the first study to evaluate the effect of bisphosphonates on inflammation in bone marrow in experimental arthritis. In our study, zoledronate treatment of rabbits with carrageenan-induced arthritis altered the histology of the bone marrow toward normal and reduced inflammation, as determined by histological assessment, regardless of whether treatment was initiated with or 2 or 4 weeks following induction of arthritis. In contrast, zoledronate treatment had no effect on synovial inflammation in rats with collagen-induced arthritis<sup>25</sup>. Synovial inflammation also remained unaltered in human TNF-transgenic mice (which develop a chronic inflammatory polyarthritis about 4–5 weeks after birth), whether the animals were treated with a single dose of zoledronate at Week 4 or repeated doses (5 times per week) over a 6-week period<sup>26</sup>. In the rat adjuvant model of arthritis, risedronate had antiinflammatory effects<sup>9,10</sup>, but pamidronate did not affect the incidence or severity of disease in collagen-induced arthritis in rats<sup>24</sup>. Finally, in collagen- and adjuvant-induced arthritis in mice, aminobisphosphonates were found to exacerbate the inflammation due to arthritis<sup>40</sup>.

Changes in PMN cells, which would represent the acute inflammatory phase, were not observed. An early study of the joint exudates in carrageenan-induced arthritis observed that the proportion of PMN cells peaks at 96% one day after a single carrageenan injection, and PMN cells are then rapidly replaced by monocytes and lymphocytes<sup>48</sup>. In our study, tissue was examined after 49 days of arthritis, well beyond the time of this peak.

The inflammation grading system we developed utilizes fundamental principles and common elements of previously developed and validated histological grading systems. These include the Knodell grading component system for evaluation of liver inflammation in hepatitis<sup>49</sup> and the semiquantitative Sydney System for classification of gastritis<sup>50</sup>. Other morphological grading systems that assign a numerical 4-level grade have been described for inflammation in the gastrointestinal tract<sup>51</sup>, eye<sup>52,53</sup>, and joint synovium<sup>25,54-57</sup>. To our knowledge, no validated system exists for the histological evaluation of inflammation in bone marrow.

Intraosseous bone marrow inflammation was observed in rat and rabbit models of experimental inflammatory arthritis. Observations performed by flow cytometry revealed the presence of an increased number of inflammatory cell types in the bone marrow in arthritic rats, and histological studies in rabbits demonstrated that bone marrow morphology is altered in inflammatory arthritis. Administration of zoledronate, a potent aminobisphosphonate, diminished the inflammatory response observed in the bone marrow in experimental arthritis and also the perforation of the tide-mark.

#### ACKNOWLEDGMENT

The authors acknowledge the contributions of Erica L. Moran and Dr. Thomas Buconjic, and the technical support of E.R. Roberts and O. Grynko. The authors thank Dagmar Gross for assistance with preparation of the manuscript. Zoledronate was provided by Novartis Pharmaceuticals Canada Ltd.

#### REFERENCES

1. Goldring SR. Bone and joint destruction in rheumatoid arthritis: what is really happening? *J Rheumatol* 2002;29 Suppl 65:44-8.
2. Bellingham CM, Lee JM, Moran EL, Bogoch ER. Bisphosphonate (Pamidronate/APD) prevents arthritis-induced loss of fracture toughness in the rabbit femoral diaphysis. *J Orthop Res* 1995;13:876-80.
3. Bogoch E, Gschwend N, Bogoch B, Rahn B, Perren S. Juxtaarticular bone loss in experimental inflammatory arthritis. *J Orthop Res* 1988;6:648-56.
4. Bogoch E, Gschwend N, Bogoch B, Rahn B, Perren S. Changes in the metaphysis and diaphysis of the femur proximal to the knee in rabbits with experimentally induced arthritis. *Arthritis Rheum* 1989;32:617-24.
5. Bogoch ER, Moran E, Crowe S, Fornasier VL. Arthritis not immobilization causes bone loss in the carrageenan injection model of inflammatory arthritis. *J Orthop Res* 1995;13:777-82.
6. Bogoch ER, Roberts EM, Moran EL, Fornasier VL. Pamidronate prevents rapid bone remodelling and rapid bone loss in experimental inflammatory arthritis. *Trans Orthop Res Soc Orthop Trans* 1996;19:1110-1.
7. Pysklywec MW, Moran EL, Fornasier VL, Bogoch ER. Altered pore characteristics and geometry in diaphyseal cortical bone affected by experimental inflammatory arthritis. *J Orthop Rheumatol* 1996;9:150-6.
8. Osterman T, Kippo K, Laruen L, Hannuniemi R, Sellman R. Effect of clodronate on established adjuvant arthritis. *Rheumatol Int* 1994;14:139-47.
9. Francis MD, Hovancik K, Boyce RW. NE-58095: A diphosphonate which prevents bone erosion and preserves joint architecture in experimental arthritis. *Int J Tissue React* 1989;11:239-52.
10. Barbier A, Brelie JC, Remandet B, Roncucci R. Studies on the chronic phase of adjuvant arthritis: effect of SR 41319, a new diphosphonate. *Ann Rheum Dis* 1986;45:67-74.
11. Osterman T, Kippo K, Lauren L, Hannuniemi R, Sellman R. Effect of clodronate on established collagen-induced arthritis in rats. *Inflamm Res* 1995;44:258-63.
12. Gravalles EM, Goldring SR. Cellular mechanisms and the role of cytokines in bone erosions in rheumatoid arthritis. *Arthritis Rheum* 2000;43:2143-51.
13. Smith RL. Degradative enzymes in osteoarthritis. *Front Biosci* 1999;4:D704-12.
14. Van Rooijen N. Extracellular and intracellular action of clodronate in osteolytic bone diseases? A hypothesis. *Calcif Tissue Int* 1993;52:407-10.
15. Van Lent PL, Holthuysen AE, van den Bersselaar L, van Rooijen N, van de Putte LB, van den Berg WB. Role of macrophage-like synovial lining cells in localization and expression of experimental arthritis. *Scand J Rheumatol* 1995;101S:83-9.
16. Jimenez-Boj E, Redlich K, Turk B, et al. Interaction between synovial inflammatory tissue and bone marrow in rheumatoid arthritis. *J Immunol* 2005;175:2579-88.
17. Gortz B, Hayer S, Redlich K, et al. Arthritis induces lymphocytic bone marrow inflammation and endosteal bone formation. *J Bone Miner Res* 2004;19:990-8.
18. Bogoch ER, Moran EL. Abnormal bone remodeling in inflammatory arthritis. *Can J Surg* 1998;41:264-71.
19. Green JR, Rogers MJ. Pharmacologic profile of zoledronic acid: a highly potent inhibitor of bone resorption. *Drug Dev Res* 2002;55:210-24.
20. Podworny NV, Kandel RA, Renlund RC, Grynpas MD. Partial chondroprotective effect of zoledronate in a rabbit model of inflammatory arthritis. *J Rheumatol* 1999;26:1972-82.
21. Pysklywec MW, Moran EL, Bogoch ER. Zoledronate, a bisphosphonate, protects against metaphyseal intracortical defects in experimental inflammatory arthritis. *J Orthop Res* 1997;15:858-61.
22. Zhao H, Shuto T, Hirata G, Iwamoto Y. Aminobisphosphonate (YM175) inhibits bone destruction in rat adjuvant arthritis. *J Orthop Sci* 2000;5:397-403.
23. Kinne RW, Schmidt-Weber CB, Hoppe R, et al. Long-term amelioration of rat adjuvant arthritis following systemic elimination of macrophages by clodronate-containing liposomes. *Arthritis Rheum* 1995;38:1777-90.
24. Markusse HM, Lafeber GJM, Breedveld FC. Bisphosphonates in collagen arthritis. *Rheumatol Int* 1990;9:281-3.
25. Sims NA, Green JR, Glatt M, et al. Targeting osteoclasts with zoledronic acid prevents bone destruction in collagen-induced arthritis. *Arthritis Rheum* 2004;50:2338-46.
26. Herrak P, Gortz B, Hayer S, et al. Zoledronic acid protects against local and systemic bone loss in tumor necrosis factor-mediated arthritis. *Arthritis Rheum* 2004;50:2327-37.
27. Moran EL, Fornasier VL, Bogoch ER. Pamidronate prevents bone loss associated with carrageenan arthritis by reducing resorptive activity but not recruitment of osteoclasts. *J Orthop Res* 2000;18:873-81.
28. Bogoch ER, Fornasier VL, Moran EL, Hansra P. Carrageenan-induced arthritis in the rat. *Inflammation* 2000;24:141-55.
29. Landis J, Koch G. The measurement of observer agreement for categorical data. *Biometrics* 1977;33:159-74.
30. Pelegri C, Franch A, Castellote C, Castell M. Immunohistochemical changes in synovial tissue during the course of adjuvant arthritis. *J Rheumatol* 1995;22:124-32.
31. Lucas S, Bogoch E, Nespeca R, Grynpas MD. Bone changes

- induced in a rabbit model of experimental arthritis. *Eur J Exp Musculoskel Res* 1992;1:121-9.
32. Massey HM, Flanagan AM. Human osteoclasts derive from CD14-positive monocytes. *Br J Haematol* 1999;106:167-70.
  33. Kong YY, Feige U, Sarosi I, et al. Activated T cells regulate bone loss and joint destruction in adjuvant arthritis through osteoprotegerin ligand. *Nature* 1999;402:304-9.
  34. Pataki A, Muller K, Green JR, Ma YF, Li QN, Jee WS. Effects of short-term treatment with the bisphosphonates zoledronate and pamidronate on rat bone: a comparative histomorphometric study on the cancellous bone formed before, during, and after treatment. *Anat Rec* 1997;249:458-68.
  35. Giuliani N, Pedrazzoni M, Passeri G, Girasole G. Bisphosphonates inhibit IL-6 production by human osteoblast-like cells. *Scand J Rheumatol* 1998;27:38-41.
  36. Hasegawa J, Nagashima M, Yamamoto M, Nishuima T, Katsumata S, Yoshino S. Bone resorption and inflammatory inhibition efficacy of intermittent cyclical etidronate therapy in rheumatoid arthritis. *J Rheumatol* 2003;30:474-9.
  37. Iwase M, Kim KJ, Kobayashi Y, Itoh M, Itoh T. A novel bisphosphonate inhibits inflammatory bone resorption in a rat osteolysis model with continuous infusion of polyethylene particles. *J Orthop Res* 2002;20:499-505.
  38. Makkonnen N, Salminen A, Rogers MJ, et al. Contrasting effects of alendronate and clodronate on RAW 264 macrophages: the role of a bisphosphonate metabolite. *Eur J Pharmacol Sci* 1999;8:109-18.
  39. Maksymowych WP. Bisphosphonates — anti-inflammatory properties. *Curr Med Chem* 2002;1:15-28.
  40. Nakamura M, Ando T, Abe M, Kumagai K, Endo Y. Contrast between effects of aminobisphosphonates and non-aminobisphosphonates on collagen-induced arthritis in mice. *Br J Pharmacol* 1996;119:205-12.
  41. Tanahashi M, Funaba Y, Itoh M, Kawabe N, Nakadate-Matsushita T. Inhibitory effects of TRK-530 on rat adjuvant arthritis. *Pharmacology* 1998;56:242-51.
  42. Tanahashi M, Koike J, Kawabe N, Nakadate-Matsushita T. Inhibitory effect of TRK-530 on inflammatory cytokines in bone marrow of rats with adjuvant arthritis. *Pharmacology* 1998;56:237-41.
  43. Van Offel JF, Schuerwegh AJ, Bridts CH, Bracke PG, Stevens WJ, De Clerck LS. Influence of cyclic intravenous pamidronate on proinflammatory monocytic cytokine profiles and bone density in rheumatoid arthritis patients treated with low dose prednisolone and methotrexate. *Clin Exp Rheumatol* 2001;19:13-20.
  44. Cantatore FP, Acquista CA, Pipitone V. Evaluation of bone turnover and osteoclastic cytokines in early rheumatoid arthritis treated with alendronate. *J Rheumatol* 1999;26:2318-23.
  45. Goldring SR, Gravallese EM. Bisphosphonates: Environmental protection for the joint? *Arthritis Rheum* 2004;50:2044-7.
  46. Eggelmeijer F, Pappoulos SE, van Paassen HC, et al. Increased bone mass with pamidronate treatment in rheumatoid arthritis. Results of a three-year randomized, double-blind trial. *Arthritis Rheum* 1996;39:396-402.
  47. Adami S, Bhalla AK, Dorizzi R, et al. The acute-phase response after bisphosphonate administration. *Calcif Tissue Int* 1987;41:326-31.
  48. Santer V, Sriratana A, Lowther DA. Carrageenin-induced arthritis: V. A morphologic study of the development of inflammation in acute arthritis. *Semin Arthritis Rheum* 1983;13:160-8.
  49. Knodell RG, Ishak KG, Black WC, et al. Formulation and application of a numerical scoring system for assessing histological activity in asymptomatic chronic active hepatitis. *Hepatology* 1981;1:431-5.
  50. Dixon MF, Genta RM, Yardley JH, Correa P. Classification and grading of gastritis: the updated Sydney System. *Am J Surg Pathol* 1996;20:1161-81.
  51. Caselli M, Gaudio M, Chiamenti CM, et al. Histologic findings and *Helicobacter pylori* in duodenal biopsies. *J Clin Gastroenterol* 1998;26:74-80.
  52. Guzey M, Karadede S, Dogan Z, Satici A. Ketorolac-tobramycin combination vs fluorometholone-tobramycin combination in reducing inflammation following phacoemulsification cataract extraction with scleral tunnel incision. *Ophthalmic Surg Lasers* 2000;31:451-6.
  53. Verma MJ, Mukaida N, Vollmer-Conna U, Matsushima K, Lloyd A, Wakefield D. Endotoxin-induced uveitis is partially inhibited by anti-IL-8 antibody treatment. *Invest Ophthalmol Vis Sci* 1999;40:2465-70.
  54. Frizziero L, Govoni E, Bacchini P. Intra-articular hyaluronic acid in the treatment of osteoarthritis of the knee: clinical and morphological study. *Clin Exp Rheumatol* 1998;16:441-9.
  55. Gynther GW, Dijkgraaf LC, Reinholt FP, Holmlund AB, Liem RS, de Bont LG. Synovial inflammation in arthroscopically obtained biopsy specimens from the temporomandibular joint: a review of the literature and a proposed histologic grading system. *J Oral Maxillofac Surg* 1998;56:1281-6.
  56. Van Ness K, Chobaz-Peclat V, Castellucci M, So A, Busso N. Plasminogen activator inhibitor type-1 deficiency attenuates murine antigen-induced arthritis. *Rheumatology Oxford* 2002;41:136-41.
  57. Fritz P, Laschner W, Saal JG, Deichsel G, Tuzcek HV, Wegner G. Histological classification of synovitis. *Zentralbl Allg Pathol* 1989;135:729-41.